Pergamon

Ann. Nucl. Energy, Vol. 24, No. 13, pp. 1035–1055, 1997
Published by Elsevier Science Ltd
PII: S0306-4549(96)00100-4 Printed in Great Britain
0306-4549/97 $17.00 + 0.00

AN ANALYTICAL BENCHMARK FOR NON-EQUILIBRIUM RADIATIVE TRANSFER IN AN ISOTROPICALLY SCATTERING MEDIUM

BINGJING SU and GORDON L. OLSON

Applied Theoretical and Computational Physics Division, Los Alamos National Laboratory, Los Alamos, NM 87545, U.S.A.

(Received 6 June 1996)

Abstract—Benchmark solutions to nontrivial radiation transport problems are crucial to the validation of transport codes. This paper gives an analytical transport solution for non-equilibrium radiative transfer in an infinite and isotropically scattering medium. The radiation source in the medium is isotropic in angle and constant in time (but only exists in a finite period of time), and is allowed to be uniformly distributed in a finite space or to be located at a point. The solution is constructed by applying the Fourier transform with respect to spatial variable and the Laplace transform with respect to temporal variable. The integration over angular variable is treated exactly. The resulting solution, as a function of space and time and in the form of a double integral, is evaluated numerically without much difficulty. Tables and figures are given for the resulting benchmark solution. Published by Elsevier Science Ltd.

INTRODUCTION

Radiative transfer problems, especially time-dependent ones, are generally very complex and have to be solved numerically. Many computer codes, employing different numerical algorithms and techniques, exist in the engineering and scientific community. For quantitative confirmation of the numerical schemes used in codes, it is desirable to have analytical benchmarks to which numerical solutions can be compared. In the context used here, an analytical benchmark means a solution representation to a radiative transfer problem for which an accurate numerical evaluation can be performed. Few analytical benchmarks exist in the field of non-equilibrium radiative transfer, and effort has been directed toward this aspect. Particularly, the non-equilibrium Marshak wave problem (Marshak, 1958), where an initially cold, semi-infinite, purely absorbing, and homogeneous medium is irradiated isotropically at the free surface, has received considerable attention. The full Marshak wave problem is nonlinear and is, therefore, mathematically intractable. Yet with several simplifying assumptions on material properties (Pomraning, 1979), it has been linearized and thus analyzed. Specifically, this problem has been

considered in the diffusion and spherical harmonic (P–1 and P–2) approximations, and the analytical solutions were obtained for the radiation and temperature fields at the free surface and for the radiation and material energy contents as functions of time (Pomraning, 1979; Pomraning and Shokair, 1981), as well as for the full radiation and temperature fields in the interior of the medium as functions of space and time (Pomraning, 1979; Su and Olson, 1996). In the transport description, Ganapol and Pomraning (1983) solved the problem using a multiple-collision approach motivated on physical grounds. After quite intensive analyses, they obtained the transport solutions for the radiation and temperature fields at the free surface and for the radiation and material energy contents, in the form of an infinite series of integrals. Such solutions were evaluated numerically by standard numerical techniques. However, they did not derive the solution for the distribution of radiation and temperature fields in the medium. Therefore, no benchmark transport results are available for the full solution to the non-equilibrium radiative transfer problem. One certainly could follow this multiple-collision approach (Ganapol and Pomraning, 1983) to derive the full solution in the interior of the medium.† However, the analysis and numerical evaluation of the solution obtained in this way would not be easy for those not familiar with the multiple collision approach.

Considering the need for benchmark transport results of radiation and temperature fields in the interior of a medium, we solve a different and mathematically simpler non-equilibrium radiative transfer problem than the foregoing Marshak wave problem in this paper. This problem corresponds to an initially cold, homogeneous, infinite, and isotropically scattering medium with an internal radiation source. The source is isotropic in angle, is restricted to be constant in time but only exists for a finite period of time, and is allowed to be uniformly distributed in a finite space or located at a point. For this problem, we can derive the full solution, as a function of space and time, in a straightforward way by using the Fourier transform with respect to spatial variable and the Laplace transform with respect to temporal variable. This method makes the exact treatment of integration over angular variable possible and yields the solution in a form of double integral. Based on this solution, analytical benchmark transport results for non-equilibrium radiative transfer are generated without difficulty.

THE PROBLEM

We consider a basic non-equilibrium radiative transfer problem, corresponding to an initially cold, homogeneous, infinite, and isotropically scattering medium with an internal radiation source in it. The coupled radiation transport and material balance equations in one dimensional plane geometry for this problem, neglecting hydrodynamic motion and heat conduction, are

$$\left(\frac{1}{c}\frac{\partial}{\partial t}+\mu\frac{\partial}{\partial z}\right)I(z,\mu,t)=\kappa_a(T)\left[\frac{1}{2}aT^4(z,t)-I(z,\mu,t)\right]+\kappa_s(T)\left[\frac{1}{2}\int_{-1}^{1}d\mu' I(z,\mu',t)-I(z,\mu,t)\right]+S(z,\mu,t), \tag{1a}$$

†It was brought to our attention by the referee that such an attempt has already been done and numerical results exist but have not been published.

$$\frac{1}{c}c_v(T)\frac{\partial T(z,t)}{\partial t} = \kappa_a(T)\left[\int_{-1}^{1} d\mu' I(z,\mu',t) - aT^4(z,t)\right], \tag{1b}$$

where z is the spatial variable ($-\infty < z < \infty$); μ is the cosine of the photon direction measured with respect to the z axis; t is the temporal variable ($-\infty < t < \infty$); I is the photon intensity; T is the local material temperature; S is the radiation source; κ_a is the absorption cross section (opacity) of material; κ_s is the scattering cross section of material; c_v is the heat capacity of material; a is the radiation constant; c is the speed of light.

For a general temperature dependence of κ_a, κ_s, and c_v, the two equations are nonlinear and thus mathematically intractable. However, if we assume that κ_a and κ_s are constants (independent of temperature) and that c_v is proportional to the cube of the temperature (Pomraning, 1979), i.e.

$$c_v = \alpha T^3,$$

then equations (1) become linear in I and T^4. As described previously (Pomraning, 1979), the sole purpose of these assumptions on material properties is to relax the physical content of the problem such that a detailed analytical solution can be obtained and thus provide a useful test problem for radiative transfer codes, since those codes are meant to handle an arbitrary temperature dependence of the material properties. The linearized equations can be rewritten as

$$\left(\varepsilon\frac{\partial}{\partial\tau} + \mu\frac{\partial}{\partial x} + 1\right) U(x,\mu,\tau) = \frac{c_a}{2}V(x,\tau) + \frac{c_s}{2}W(x,\tau) + Q(x,\mu,\tau), \tag{2a}$$

$$\frac{\partial V(x,\tau)}{\partial\tau} = c_a[W(x,\tau) - V(x,\tau)], \tag{2b}$$

where

$$\kappa \equiv \kappa_a + \kappa_s, \quad x \equiv \kappa z, \quad \varepsilon \equiv \frac{4a}{\alpha}, \quad \tau \equiv \varepsilon c\kappa t, \quad c_a \equiv \frac{\kappa_a}{\kappa}, \quad c_s \equiv \frac{\kappa_s}{\kappa},$$

$$U(x,\mu,\tau) \equiv \frac{I(z,\mu,t)}{aT_H^4}, \qquad V(x,\tau) \equiv \left[\frac{T(z,t)}{T_H}\right]^4,$$

$$W(x,\tau) \equiv \int_{-1}^{1} d\mu U(x,\mu,\tau), \qquad Q(x,\mu,\tau) \equiv \frac{S(z,\mu,t)}{aT_H^4},$$

with T_H being the Hohlraum temperature (or any reference temperature). In equations (2), x and τ are the scaled spatial and temporal variables; and U, W, V, and Q are the scaled radiation intensity, radiation energy density, material energy density, and radiation source, respectively. The material properties are represented by c_a, c_s, and ε, with

$c_a + c_s = 1$ and ε being an arbitrary constant. The boundary and initial conditions on equations (2a) and (2b) are

$$\lim_{x\to\pm\infty} U(x,\mu,\tau) = 0; \quad U(x,\mu,\tau) = V(x,\tau) = 0, \quad \tau < 0. \tag{2c}$$

These conditions imply that the material is initially cold (temperature equals to zero) and suffers no irradiation before the primary source $Q(x,\mu,\tau)$ is turned on at $\tau = 0$. We specifically consider, in this paper, a unit radiation source which is constant in time but only exists in a finite period of time ($0 \le \tau \le \tau_0$), isotropically distributed in angle, and uniformly distributed in a finite space ($-x_0 \le x \le x_0$), i.e.

$$Q(x,\mu,\tau) = \frac{1}{2} Q_1(x) Q_2(\tau), \tag{3}$$

with

$$Q_1(x) = \frac{1}{2x_0}[\theta(x+x_0) - \theta(x-x_0)],$$

$$Q_2(\tau) = \theta(\tau) - \theta(\tau-\tau_0).$$

Here θ is the Heaviside (unit step) function. As x_0 approaches zero, we have

$$\lim_{x_0\to 0} Q_1(x) = \delta(x).$$

That is, the source represented by $Q_1(x)$ becomes a plane source located at $x = 0$ when setting $x_0 = 0$. The reason that we do not take $Q_1(x)$ as a delta function directly is to avoid the possible difficulty of simulating a delta function numerically in real codes. Also, we keep the source on for only a limited period of time. Because if τ_0 was taken as ∞, then for the equilibrium state at large τ, the equation for radiation would become [see equations (2a) and (2b)]

$$\left(\varepsilon\frac{\partial}{\partial\tau} + \mu\frac{\partial}{\partial x} + 1\right) U(x,\mu,\tau) = \frac{1}{2} W(x,\tau) + \frac{1}{2} Q_1(x)\theta(\tau),$$

which has no finite steady-state solution since it represents a situation with a constant source but no absorption (Case *et al.*, 1953).

It should be pointed out that the whole space problem we just described can actually be treated as a half-space problem. Because the source is isotropically distributed in angle and located symmetrically around $x = 0$, the problem we are considering has symmetry with respect to the x axis. Consequently, there is no net energy flux at $x = 0$. Therefore, this full-space problem is equivalent to the half-space problem defined still by equations (2) and (3), but only for $0 \le x < \infty$ and with a reflective boundary condition at $x = 0$ given by

$$U(0,\mu,\tau) = U(0,-\mu,\tau).$$

The mathematical objective for equations (2) is to derive the analytical solutions for $W(x,\tau)$ and $V(x,\tau)$. From equation (2b) and the initial condition given by equation (2c), it is deduced that

$$V(x,\tau) = c_a \int_0^\tau d\tau' \, e^{-c_a(\tau-\tau')} \, W(x,\tau'). \tag{4}$$

Using equations (3) and (4) in equation (2a) yields the closed equation for $U(x,\mu,\tau)$

$$\left(\varepsilon\frac{\partial}{\partial\tau} + \mu\frac{\partial}{\partial x} + 1\right) U(x,\mu,\tau) = \frac{c_a^2}{2}\int_0^\tau d\tau' \, e^{-c_a(\tau-\tau')} \, W(x,\tau') + \frac{c_s}{2} W(x,\tau) + \frac{1}{2} Q_1(x) Q_2(\tau). \tag{5a}$$

The appropriate limiting conditions at $x \to \pm\infty$ and the initial condition for equation (5a) are

$$\lim_{x\to\pm\infty} U(x,\mu,\tau) = U(x,\mu,\tau<0) = 0. \tag{5b}$$

We let $\psi(x,\mu,\tau)$ denote the solution to the auxiliary problem of equations (5), corresponding to an impulsed source at $\tau = 0$, given by

$$\left(\varepsilon\frac{\partial}{\partial\tau} + \mu\frac{\partial}{\partial x} + 1\right) \psi(x,\mu,\tau) = \frac{c_a^2}{2}\int_0^\tau d\tau' \, e^{-c_a(\tau-\tau')} \, \rho(x,\tau') + \frac{c_s}{2}\rho(x,\tau) + \frac{1}{2} Q_1(x)\delta(\tau), \tag{6a}$$

$$\lim_{x\to\pm\infty} \psi(x,\mu,\tau) = \psi(x,\mu,\tau<0) = 0, \tag{6b}$$

where

$$\rho(x,\tau) = \int_{-1}^{1} d\mu \psi(x,\mu,\tau).$$

Then $U(x,\mu,\tau)$ can be expressed as [see Ganapol (1979) and Ganapol and Pomraning (1983) for the relationship between the solution corresponding to an impulsed boundary condition/source at $\tau = 0$ and that corresponding to a continuously incident boundary condition/source]

$$U(x,\mu,\tau) = \int_{\tau^*}^{\tau} d\tau' \, \psi(x,\mu,\tau'),$$

or, after integrating over μ, $W(x,\tau)$ is given by

$$W(x,\tau) = \int_{\tau^*}^{\tau} d\tau' \, \rho(x,\tau'), \tag{7}$$

where

$$\tau^* = \max[0, (\tau - \tau_0)].$$

Besides the radiation and material energy densities denoted by $W(x,\tau)$ and $V(x, \tau)$, other physically interesting quantities are the radiation and material energy contents of the infinite medium defined as

$$\phi_r(\tau) = \int_{-\infty}^{\infty} dx W(x, \tau), \qquad \phi_m(\tau) = \int_{-\infty}^{\infty} dx V(x, \tau).$$

Integrating equations (7) and (4) over x leads to

$$\phi_r(\tau) = \int_{\tau^*}^{\tau} d\tau' \phi(\tau'), \tag{8}$$

$$\phi_m(\tau) = c_a \int_0^{\tau} d\tau' \, e^{-c_a(\tau-\tau')} \phi_r(\tau'). \tag{9}$$

In equation (8), we have used

$$\phi(\tau) = \int_{-\infty}^{\infty} dx \rho(x, \tau). \tag{10}$$

Obviously, we need $\rho(x,\tau)$ and $\phi(\tau)$ to compute $W(x,\tau)$, $V(x, \tau)$, $\phi_r(\tau)$, and $\phi_m(\tau)$.

SOLUTION TO THE PROBLEM

It is usually a normal approach to derive solutions to different transport problems (either time-independent or time-dependent) in infinite medium with sources by applying the method of Case (Case, 1960; Case and Zweifel, 1967). However, using the Case method to solve the non-equilibrium problem described in the previous section would be complicated and would end up with the solutions for $W(x,\tau)$ and $V(x,\tau)$ in the form of triple integrals, which make numerical evaluation very difficult and expensive. An alternative approach was suggested by Papmehl (1966) and he demonstrated that in a time-dependent neutron transport context [without the first term in the right hand side of equation (6a)], a solution can be constructed in a simple manner by using a double Fourier transform with respect to both temporal and spatial variables. However, applying the Fourier transform in the temporal variable to problems with initial conditions at $\tau < 0$, such as equations (6), may be invalid. For some problems, such treatment yields wrong solutions. In his work, Papmehl actually did not prove the validity of applying the Fourier transform in the time variable, that is bounded for $\tau \geq 0$, to his problem. Here, we use a slightly different method than Papmehl's to treat our problem: we apply the Fourier transform with respect to the unbounded spatial variable and apply the Laplace transform with respect to the bounded temporal variable to obtain the solutions for $\rho(x, \tau)$ and $\phi(\tau)$. Specifically, we introduce the double transform according to

$$\bar{f}(k, s) = \int_0^{\infty} d\tau e^{-s\tau} \int_{-\infty}^{\infty} dx e^{-ikx} f(x, \tau) \tag{11}$$

to equations (6). Here s is a complex variable and k is a real variable. Multiplying equation (6a) by $\exp[-(ikx + s\tau)]$, integrating over x and τ (interchanging integration orders of τ and τ' for the first right hand side term), and using equation (6b) yields

$$(1 + \varepsilon s + i\mu k)\bar{\psi}(k, \mu, s) = \frac{1}{2}\left[\frac{c_a^2}{(c_a + s)} + c_s\right]\bar{\rho}(k, s) + \frac{1}{2}\bar{Q}_1(k), \tag{12}$$

where

$$\bar{Q}_1(k) = \int_{-\infty}^{\infty} \mathrm{d}x\, \mathrm{e}^{-ikx} Q_1(x) = \begin{cases} \dfrac{\sin(kx_0)}{kx_0}, & x_0 \neq 0, \\ 1, & x_0 = 0. \end{cases}$$

Note that $x_0 = 0$ implies that $Q_1(x)$ is a delta function, as discussed in the previous section. Dividing equation (12) by $(1 + \varepsilon s + i\mu k)$, integrating over μ from -1 to 1, and solving for $\bar{\rho}(k,s)$ (using $c_a + c_s = 1$), we obtain

$$\bar{\rho}(k, s) = \frac{(c_a + s)b(k, s)\bar{Q}_1(k)}{[(c_a + s) - b(k, s)(c_a + c_s s)]}, \tag{13}$$

with $b(k,s)$ being defined as

$$b(k, s) = \frac{1}{2}\int_{-1}^{1} \frac{\mathrm{d}\mu}{(1 + \varepsilon s + i\mu k)}. \tag{14}$$

The function $\phi(\tau)$, defined by equation (10), can be found very easily by setting $k = 0$ in the transform equation for $\rho(x,\tau)$. Based on equations (11) and (10), we have

$$\bar{\rho}(0, s) = \int_0^{\infty} \mathrm{d}\tau\, \mathrm{e}^{-s\tau} \int_{-\infty}^{\infty} \mathrm{d}x \rho(x, \tau) = \int_0^{\infty} \mathrm{d}\tau\, \mathrm{e}^{-s\tau} \phi(\tau). \tag{15}$$

This equation states that the Laplace transform (in τ) of $\phi(\tau)$ simply equals $\bar{\rho}(0,s)$. Then, $\phi(\tau)$ is given by the Laplace inverse transform of $\bar{\rho}(0,s)$. Setting $k = 0$ in equation (13) gives

$$\bar{\rho}(0, s) = \frac{c_a + s}{s[\varepsilon s + c_a(1 + \varepsilon)]} = \frac{1}{(1 + \varepsilon)s} + \frac{1}{\varepsilon(1 + \varepsilon)[s + c_a(1 + \varepsilon)/\varepsilon]}.$$

Thus, inverting $\bar{\rho}(0,s)$ back to the τ domain, we obtain

$$\phi(\tau) = \frac{1}{(1 + \varepsilon)} + \frac{1}{\varepsilon(1 + \varepsilon)}\, \mathrm{e}^{-c_a(1+\varepsilon)\tau/\varepsilon}. \tag{16}$$

We see that $\phi(\tau)$ has a very simple expression and is independent of the spatial distribution of the source (x_0). One could prove easily that this result is also true for any

anisotropic (in angle) source. Physically, this means that no matter where and in which direction the impulsed source is, it yields a same energy content throughout the infinite medium.

To obtain the solution for $\rho(x,\tau)$, we first consider the Laplace inversion of $\bar{\rho}(k,s)$ and have

$$\rho(k,\tau)=\frac{1}{2\pi i}\int_C \mathrm{d}s\,\frac{(c_a+s)b(k,s)\bar{Q}_1(k)\mathrm{e}^{s\tau}}{[(c_a+s)-b(k,s)(c_a+c_s s)]}, \tag{17}$$

where the integration contour C is a line parallel to the imaginary s axis to the right of all the singularities of the integrand. For a fixed and real parameter k, the poles of the integrand are the roots of the equation given by

$$b(k,s)=\frac{c_a+s}{c_a+c_s s}=1+\frac{c_a s}{c_a+c_s s}. \tag{18}$$

We cannot find the roots of equation (18) explicitly. However, we can prove that the roots are in the left half space of s, i.e. $\mathrm{Re}(s^*)<0$, where s^* are the roots of equation (18). Because, if $\mathrm{Re}(s^*)>0$, the modulus of the right hand side of equation (18) is obviously greater than unity and the modulus of the left hand side of the equation is smaller than unity according to equation (14). This makes the equality impossible. Thus, no poles exist in the right half space of s. In addition to these poles, the integrand also has two branch cuts, due to $b(k,s)$, in the left half space of s, with branch points at $s=-(1\pm ik)/\varepsilon$. We, therefore, conclude that there are no singularities in the right half s-plane because the Fourier transform is applied to the spatial variable. This fact is quite different from other similar analyses for related problems, such as that given by Kuščer and Zweifel (1965), where the spatial variable is treated differently. Since all the singularities of the integrand are in the left half space of s, the integration contour C in equation (17) is then taken as the imaginary axis of s and the integration variables are changed accordingly from s to $i\omega$, with ω being a real variable. We thus have

$$\rho(k,\tau)=\frac{1}{2\pi}\int_{-\infty}^{\infty}\mathrm{d}\omega\,\frac{(c_a+i\omega)b(k,\omega)\bar{Q}_1(k)\,\mathrm{e}^{i\omega\tau}}{[(c_a+i\omega)-b(k,\omega)(c_a+ic_s\omega)]}, \tag{19}$$

where now

$$b(k,\omega)=\frac{1}{2}\int_{-1}^{1}\frac{\mathrm{d}\mu}{[1+i(\varepsilon\omega+\mu k)]}. \tag{20}$$

After the Fourier inversion of equation (19) with respect to the variable k, $\rho(x,\tau)$ is given by

$$\rho(x,\tau)=\frac{1}{(2\pi)^2}\int_{-\infty}^{\infty}\mathrm{d}k\int_{-\infty}^{\infty}\mathrm{d}\omega\,\frac{(c_a+i\omega)b(k,\omega)\bar{Q}_1(k)\,\mathrm{e}^{i(kx+\omega\tau)}}{[(c_a+i\omega)-b(k,\omega)(c_a+ic_s\omega)]}. \tag{21}$$

In fact, equation (21) could have been obtained directly by applying the double Fourier transform (from x and τ to k and ω) to equation (6a), solving for $\bar{p}$, and using the Fourier inversion theorem, just as what Papmehl did to the neutron transport equation (Papmehl, 1966). Yet the validity of using the double Fourier transform method to our problem would then have not been clear. For the problem under consideration, the Fourier transform in τ is equivalent to the Laplace transform in τ simply because that the integration contour in the Laplace inversion can be taken as the pure imaginary axis. Thus, using the double Fourier transform method directly is valid. However, not all time-dependent problems with initial conditions share this property.

It is very unlikely to perform the double integral given in equation (21) analytically due to the existence of $b(k,\omega)$. Accordingly, we explicitly manipulate equation (21) into an expression that is suitable to be calculated numerically. Performing the integration given by equation (20) yields

$$b(k, \omega) = p(k, \omega) - iq(k, \omega), \tag{22}$$

where

$$p(k, \omega) = \frac{1}{2}\int_{-1}^{1} \frac{\mathrm{d}\mu}{1 + (\varepsilon\omega + \mu k)^2} = \frac{1}{2k}[\tan^{-1}(k + \varepsilon\omega) + \tan^{-1}(k - \varepsilon\omega)], \tag{23a}$$

$$q(k, \omega) = \frac{1}{2}\int_{-1}^{1} \frac{(\varepsilon\omega + \mu k)\,\mathrm{d}\mu}{1 + (\varepsilon\omega + \mu k)^2} = \frac{1}{2k}\tanh^{-1}\left(\frac{2\varepsilon\omega k}{1 + \varepsilon^2\omega^2 + k^2}\right). \tag{23b}$$

Inserting equation (22) in equation (21) and separating the real and imaginary parts, we have

$$\rho(x, \tau) = \frac{1}{(2\pi)^2}\int_{-\infty}^{\infty} \mathrm{d}k \int_{-\infty}^{\infty} \mathrm{d}\omega\,[h(k, \omega) - ig(k, \omega)]\,\mathrm{e}^{i(kx+\omega\tau)}, \tag{24}$$

in which we have defined

$$h(k, \omega) = \frac{\overline{Q}_1(k)}{r(k, \omega)}[(c_a^2 + \omega^2)p - (c_a^2 + c_s\omega^2)(p^2 + q^2)], \tag{25a}$$

$$g(k, \omega) = \frac{\overline{Q}_1(k)}{r(k, \omega)}[(c_a^2 + \omega^2)q + c_a^2\omega(p^2 + q^2)], \tag{25b}$$

and

$$r(k, \omega) = (c_a^2 + c_s^2\omega^2)(p^2 + q^2) + 2c_a^2\omega q - 2(c_a^2 + c_s\omega^2)p + \omega^2 + c_a^2. \tag{25c}$$

Expanding the exponential term in equation (24) as

$$\mathrm{e}^{i(kx+\omega\tau)} = \cos(kx + \omega\tau) + i\sin(kx + \omega\tau)$$

leads to

$$\rho(x,\tau)=\frac{1}{(2\pi)^2}\int_{-\infty}^{\infty}\mathrm{d}k\int_{-\infty}^{\infty}\mathrm{d}\omega\,[\cos(kx+\omega\tau)\cdot h(k,\omega)+\sin(kx+\omega\tau)\cdot g(k,\omega)]$$
$$+\frac{i}{(2\pi)^2}\int_{-\infty}^{\infty}\mathrm{d}k\int_{-\infty}^{\infty}\mathrm{d}\omega\,[\sin(kx+\omega\tau)\cdot h(k,\omega)-\cos(kx+\omega\tau)\cdot g(k,\omega)]. \tag{26}$$

Equation (26) is the expression for $\rho(x,\tau)$, with real and imaginary parts being separated. Based on physical consideration, the imaginary part should be equal to zero. It is easy to show that this is the case. If a function $f(k,\omega)$ is symmetric with respect to the origin of coordinates, the following rule applies

$$\int_{-\infty}^{\infty}\mathrm{d}k\int_{-\infty}^{\infty}\mathrm{d}\omega\,f(k,\omega)=$$
$$\begin{cases}0, & \text{if } f(-k,-\omega)=-f(k,\omega) \text{ or odd symmetry,}\\ 2\displaystyle\int_{0}^{\infty}\mathrm{d}k\int_{-\infty}^{\infty}\mathrm{d}\omega\,f(k,\omega), & \text{if } f(-k,\omega)=f(k,\omega) \text{ or even symmetry.}\end{cases}$$

It is easy to verify that $h(k,\omega)$ and $\cos(kx+\omega\tau)$ have even symmetry, whereas $g(k,\omega)$ and $\sin(kx+\omega\tau)$ have odd symmetry, with respect to the origin. These lead to the result that both the imaginary terms of the integrand in equation (26) are odd functions, and both the real terms are even functions, with respect to the origin. Then, according to the foregoing rule, equation (26) reduces to

$$\rho(x,\tau)=\frac{1}{2\pi^2}\int_{0}^{\infty}\mathrm{d}k\int_{-\infty}^{\infty}\mathrm{d}\omega\,[\cos(kx+\omega\tau)\cdot h(k,\omega)+\sin(kx+\omega\tau)\cdot g(k,\omega)]. \tag{27}$$

This result can be further simplified. From equations (23) and (25), we see that p, q, r, h, and g are also symmetric with respect to the ω axis. Specifically, p, r, and h are even functions in ω, and q and g are odd functions in ω. After expanding the trigonometric functions in equation (27) as

$$\cos(kx+\omega\tau)=\cos(kx)\cos(\omega\tau)-\sin(kx)\sin(\omega\tau),$$

$$\sin(kx+\omega\tau)=\sin(kx)\cos(\omega\tau)+\cos(kx)\sin(\omega\tau),$$

the odd terms in ω of the integrand, that contribute zero to the integration over ω from $-\infty$ to ∞, are deleted. For the remaining even terms in ω, the integration range of ω can be reduced to a half-space, thus equation (27) becomes

$$\rho(x,\tau)=\frac{1}{\pi^2}\int_{0}^{\infty}\mathrm{d}k\int_{0}^{\infty}\mathrm{d}\omega\cos(kx)[h(k,\omega)\cos(\omega\tau)+g(k,\omega)\sin(\omega\tau)]. \tag{28}$$

Equation (28) is the solution, in the form of a double integral, to equations (6) which correspond to an impulsed source at $\tau = 0$. As expected, this result is symmetric with respect to x axis since the source is isotropic in angle and located symmetrically around $x = 0$. The double integral in equation (28) cannot be done analytically. However, its integration over x has a very simple expression given by equation (16).

With $\phi(\tau)$ and $\rho(x,\tau)$ obtained, it is easy to construct the solution to the problem. We first consider the total energy contents in the infinite medium. Inserting equation (16) in equation (8), then inserting the resulting solution for ϕ_r in equation (9), and carrying out the algebra, we obtain the radiation and material energy contents to be

$$\phi_r(\tau) = \begin{cases} \dfrac{\tau}{(1+\varepsilon)} + \dfrac{1}{c_a(1+\varepsilon)^2}\left[1 - e^{-c_a(1+\varepsilon)\tau/\varepsilon}\right], & \tau \le \tau_0, \\ \dfrac{\tau_0}{(1+\varepsilon)} + \dfrac{1}{c_a(1+\varepsilon)^2}\left[e^{-c_a(1+\varepsilon)(\tau-\tau_0)/\varepsilon} - e^{-c_a(1+\varepsilon)\tau/\varepsilon}\right], & \tau > \tau_0, \end{cases} \tag{29}$$

$$\phi_m(\tau) = \begin{cases} \dfrac{\tau}{(1+\varepsilon)} - \dfrac{\varepsilon}{c_a(1+\varepsilon)^2}\left[1 - e^{-c_a(1+\varepsilon)\tau/\varepsilon}\right], & \tau \le \tau_0, \\ \dfrac{\tau_0}{(1+\varepsilon)} - \dfrac{\varepsilon}{c_a(1+\varepsilon)^2}\left[e^{-c_a(1+\varepsilon)(\tau-\tau_0)/\varepsilon} - e^{-c_a(1+\varepsilon)\tau/\varepsilon}\right], & \tau > \tau_0. \end{cases} \tag{30}$$

These results are actually independent of the spatial and angular distribution of the internal source. Therefore, equations (29) and (30) are valid for any arbitrary source as long as the total source strength is one. Also, it is found, from equations (29) and (30), that $\phi_r(\tau)$ and $\phi_m(\tau)$ satisfy

$$\varepsilon\phi_r(\tau) + \phi_m(\tau) = \begin{cases} \tau, & \tau \le \tau_0, \\ \tau_0, & \tau > \tau_0. \end{cases} \tag{31}$$

We see that the sum of the energy contents increases linearly with τ when the source is on and is constant after the source is turned off.

Similarly, using equation (28) in equation (7) and then using the result in equation (4) yields the following solutions for the radiation and material energy densities in the medium, as functions of space and time,

$$W(x,\tau) = \frac{1}{\pi^2}\int_0^\infty dk \int_0^\infty d\omega \frac{\cos(kx)}{\omega}\{h \cdot \sin(\omega\tau) + g \cdot [1 - \cos(\omega\tau)]\}, \quad \tau \le \tau_0, \tag{32a}$$

$$W(x,\tau) = \frac{1}{\pi^2}\int_0^\infty dk \int_0^\infty d\omega \frac{\cos(kx)}{\omega}\{h \cdot [\sin(\omega\tau) - \sin\omega(\tau - \tau_0)] + g \cdot [\cos\omega(\tau - \tau_0) - \cos(\omega\tau)]\}, \quad \tau > \tau_0, \tag{32b}$$

$$V(x,\tau) = W(x,\tau) - \frac{1}{\pi^2}\int_0^\infty dk \int_0^\infty d\omega \frac{\cos(kx)}{(c_a^2+\omega^2)}\{(\omega h + c_a g)\cdot \sin(\omega\tau) + (c_a h - \omega g)\cdot[\cos(\omega\tau) - e^{-c_a\tau}]\}, \quad \tau \le \tau_0, \tag{33a}$$

$$V(x,\tau) = W(x,\tau) - \frac{1}{\pi^2}\int_0^\infty dk \int_0^\infty d\omega \frac{\cos(kx)}{(c_a^2+\omega^2)}\{(\omega h + c_a g)\cdot[\sin(\omega\tau) - \sin\omega(\tau-\tau_0)] + (c_a h - \omega g)\cdot[\cos(\omega\tau) - \cos\omega(\tau-\tau_0) + e^{-c_a(\tau-\tau_0)} - e^{-c_a\tau}]\}, \quad \tau > \tau_0. \tag{33b}$$

where h and g, as functions of k and ω, are defined by equations (25). These solutions are all in the form of double integrals and have to be evaluated numerically. The numerical evaluation of these solutions is not exceptionally difficult, although not trivial. The details of the numerical investigation of these solutions and the numerical results are given in a later section.

ASYMPTOTIC APPROXIMATIONS

In this section, we consider the asymptotic approximations for the solutions. We first derive the asymptotic solution for $W(x,\tau)$ at large τ. Substituting equation (21) in equation (7), we have the exact expression for $W(x,\tau)$ at $\tau > \tau_0$,

$$W(x,\tau) = \frac{1}{(2\pi)^2}\int_{-\infty}^\infty dk \int_{-\infty}^\infty d\omega \frac{(c_a+i\omega)b(k,\omega)\overline{Q}_1(k)e^{i(kx+\omega\tau)}}{[(c_a+i\omega) - b(k,\omega)(c_a+ic_s\omega)]}\left(\frac{1-e^{-i\omega\tau_0}}{i\omega}\right). \tag{34}$$

For large times ($\tau \gg \tau_0$), the main contribution to the integral over ω is due to the small values of ω. Hence, we can expand $b(k,\omega)$ and the last term in equation (34) around $\omega = 0$. Neglecting quadratic and higher terms in ω, we obtain [see equations (22) and (23)]

$$b(k,\omega) \approx p_a(k) - i\omega q_a(k), \tag{35}$$

where

$$p_a(k) = \frac{1}{k}\tan^{-1}(k), \qquad q_a(k) = \frac{\varepsilon}{1+k^2},$$

and

$$\left(\frac{1-e^{-i\omega\tau_0}}{i\omega}\right) \approx \tau_0\left(1 - \frac{1}{2}i\tau_0\omega\right). \tag{36}$$

Using equations (35) and (36) in equation (34) and only keeping the linear terms in ω (note here it is assumed that $c_a \neq 0$ otherwise the quadratic terms should be kept) yields the equation for the asymptotic solution, that is denoted by $W_a(x,\tau)$ here, given by

$$W_a(x,\tau) = \frac{\tau_0}{(2\pi)^2}\int_{-\infty}^\infty dk\, e^{ikx}\overline{Q}_1(k)\int_{-\infty}^\infty d\omega \frac{[c_a p_a + i\omega(p_a - c_a q_a - c_a p_a\tau_0/2)]e^{i\omega\tau}}{[c_a(1-p_a) + i\omega(1 + c_a q_a - c_s p_a)]}. \tag{37}$$

The integral of ω can be evaluated analytically by a simple contour integration. As a result, we have

$$W_a(x,\tau)=\frac{\tau_0}{2\pi}\int_{-\infty}^{\infty}dk\,e^{ikx}\,\overline{Q}_1(k)\,\frac{c_a^2[(1-\tau_0/2)p_a^2+\tau_0 p_a/2+q_a]\,e^{-\omega^*\tau}}{(1+c_a q_a-c_s p_a)^2},\tag{38}$$

where

$$\omega^*=\frac{c_a(1-p_a)}{1+c_a q_a-c_s p_a}.$$

We see that $\omega^*=0$ at $k=0$, thus the integrand of equation (38) is peaked at $k=0$ and the main contribution to this integral comes from small values of k when τ is large enough. Expanding p_a, q_a, ω^*, and $\overline{Q}_1(k)$ in terms of k as

$$p_a\approx 1-\frac{1}{3}k^2,\qquad q_a\approx\varepsilon(1-k^2),\qquad \omega^*\approx\frac{1}{3(1+\varepsilon)}k^2,\qquad \overline{Q}_1(k)\approx 1-\frac{1}{3}x_0^2k^2,$$

inserting these results in equation (38), and omitting higher than quadratic terms lead to

$$W_a(x,\tau)=\frac{\tau_0}{2\pi(1+\varepsilon)}\int_{-\infty}^{\infty}dk\left[1+\frac{2\beta}{3(1+\varepsilon)}k^2\right]\exp\left[ikx-\frac{\tau}{3(1+\varepsilon)}k^2\right],\tag{39}$$

where the parameter β is given by

$$\beta=\frac{3\varepsilon}{2}-\frac{1}{c_a}+\frac{\tau_0}{4}-\frac{1}{2}(1+\varepsilon)x_0^2.$$

Manipulating the integral in equation (39) explicitly yields the asymptotic time–space distribution at large times as

$$W_a(x,\tau)=\frac{\tau_0}{2}\sqrt{\frac{3}{\pi(1+\varepsilon)\tau}}\left[1+\frac{\beta}{\tau}-\frac{3\beta(1+\varepsilon)x^2}{2\tau^2}\right]\exp\left[-\frac{3(1+\varepsilon)x^2}{4\tau}\right].\tag{40}$$

Equation (40) is the asymptotic approximation to equation (32b) at large times. Integration of equation (40) over x from $-\infty$ to ∞ gives

$$\phi_{r,a}(\tau)=\int_{-\infty}^{\infty}dx\,W_a(x,\tau)=\frac{\tau}{(1+\varepsilon)},\tag{41}$$

which agrees with the leading term of the exact result given by equation (29) when $\tau\gg\tau_0$. Following the same procedure or simply utilizing equation (40) in equation (4) [in which $W(x,\tau)$ at any τ can be reasonably approximated by $W_a(x,\tau)$ due to the fact that the

contribution to that integral at small τ is negligible], one could also derive the asymptotic approximation for $V(x,\tau)$ at large times. However, such pursuit is unnecessary, since at large times $V(x,\tau)$ and $W(x,\tau)$ are almost identical.

We next consider the small τ approximations. Converting $\overline{\rho}(k,s)$ [given by equation (13)] back to the x and τ domains yields

$$\rho(x,\tau) = \mathcal{F}^{-1}\left\{\overline{Q}_1(k)\mathcal{L}^{-1}\left[\frac{(c_a+s)b(k,s)}{(c_a+s)-b(k,s)(c_a+c_s s)}\right]\right\}, \tag{42}$$

where $\mathcal{F}^{-1}$ and $\mathcal{L}^{-1}$ represent the inverse Fourier transform operator and the inverse Laplace transform operator, respectively. Since small τ corresponds to large s, we expand $b(k,s)$ defined by equation (14), at large s, as

$$b(k,s) = \frac{1}{2}\int_{-1}^{1} d\mu \left[\frac{1}{\varepsilon s} - \frac{(1+i\mu k)}{(\varepsilon s)^2} + \cdots\right] = \frac{1}{\varepsilon s} - \frac{1}{(\varepsilon s)^2} + \cdots \tag{43}$$

We then use equation (43) in equation (42) and further simplify the expression as

$$\rho(x,\tau) \approx \mathcal{F}^{-1}[\overline{Q}_1(k)]\mathcal{L}^{-1}\left[\frac{(\varepsilon s - c_a)}{(\varepsilon s)^2}\right] = Q_1(x)\left[\frac{1}{\varepsilon} - \frac{c_a\tau}{\varepsilon^2}\right]. \tag{44}$$

Using this result in equations (7) and (4), we obtain the small τ approximations for energy densities, denoted here as $W_s(x,\tau)$ and $V_s(x,\tau)$,

$$W_s(x,\tau) = Q_1(x)\left[\frac{\tau}{\varepsilon} - \frac{c_a\tau^2}{2\varepsilon^2}\right], \qquad V_s(x,\tau) = Q_1(x)\left[\frac{c_a\tau^2}{2\varepsilon}\right], \tag{45}$$

with errors in the order of τ^3. It is easy to verify that the temporal behaviors of $W_s(x,\tau)$ and $V_s(x,\tau)$, after integration over x, agree with equations (29) and (30) up to the quadratic terms for small τ. This small τ asymptotic solution, together with the large τ asymptotic solution, can be used to validate whatever numerical schemes that will be used to evaluate the double integrals derived in the previous section by comparing numerical results with the prediction of these asymptotic solutions. It should be noted that equation (45) is only a preliminary approximation and it indicates that at very small times, the radiation and material energy densities only depend upon the local source. The effect of streaming is totally neglected because only the first two terms, that are independent of k, are kept in the expansion of $b(k,s)$. Neglecting the streaming effect is justifiable for spatial positions well within the source region, where the spatial gradients of densities are very small. However, this is not the case near the edges of the source region (note that the source is uniformly distributed in $-x_0 \le x \le x_0$), where the spatial gradients of densities are huge and thus the effect of streaming is important. Therefore, equation (45) is not valid near $\pm x_0$. To derive better small τ approximations, one should keep higher terms to include the variable k in the expansion of $b(k,s)$ and treat the poles of the inverse Laplace transform as functions of k. However, such treatment would prevent one from obtaining explicit results in elementary functions.

NUMERICAL RESULTS

The evaluation of the integrals in equations (32) and (33) proceeds in a manner very similar to the process outlined in an earlier paper (Su and Olson, 1996). The w–k plane is divided into areas whose sides are chosen to be multiples of π. Farther from the origin, as the contribution to the integrals decreases, larger areas are chosen. Each area is evaluated using the multiple integral method discussed in Section 4.6 of the book *Numerical Recipes in Fortran* (Press *et al.*, 1992). Each one-dimensional integral is evaluated with the open Romberg method to a specified accuracy. However, when the inner one-dimensional integrals are added to compute the two dimensional integral, the cancellation due to the oscillation of the integrand causes the tolerances for the one-dimensional integrals to be almost useless for quantifying the accuracy of final results. Therefore, we adopted the conservative approach of tightening the error tolerances for the integrals in each area until the final result for W and V at each evaluated point was converged to at least 1×10^{-4}. That is, we required as a minimum that the first four digits after the decimal point were

Table 1. Radiation energy density, $W(x,\tau)$, for the case with $\varepsilon = 1$, $c_a = 1$, $\tau_0 = 10$, $x_0 = 0.5$. The upper section is diffusion solution and the lower section is transport solution

$x \setminus \tau$	0.10000	0.31623	1.00000	3.16228	10.0000	31.6228	100.000
0.01000	0.09403	0.24356	0.50359	0.95968	1.86585	0.66600	0.35365
0.10000	0.09326	0.24002	0.49716	0.95049	1.85424	0.66562	0.35360
0.17783	0.09128	0.23207	0.48302	0.93036	1.82889	0.66479	0.35347
0.31623	0.08230	0.20515	0.43743	0.86638	1.74866	0.66216	0.35309
0.45000	0.06086	0.15981	0.36656	0.76956	1.62824	0.65824	0.35252
0.50000	0.04766	0.13682	0.33271	0.72433	1.57237	0.65643	0.35225
0.56234	0.03171	0.10856	0.29029	0.66672	1.50024	0.65392	0.35188
0.75000	0.00755	0.05086	0.18879	0.51507	1.29758	0.64467	0.35051
1.00000	0.00064	0.01583	0.10150	0.35810	1.06011	0.62857	0.34809
1.33352		0.00244	0.04060	0.21309	0.79696	0.60098	0.34382
1.77828			0.01011	0.10047	0.52980	0.55504	0.33636
3.16228			0.00003	0.00634	0.12187	0.37660	0.30185
5.62341					0.00445	0.11582	0.21453
10.00000						0.00384	0.07351
17.78279							0.00269
0.01000	0.09531	0.27526	0.64308	1.20052	2.23575	0.69020	0.35720
0.10000	0.09531	0.27526	0.63585	1.18869	2.21944	0.68974	0.35714
0.17783	0.09532	0.27527	0.61958	1.16190	2.18344	0.68878	0.35702
0.31623	0.09529	0.26262	0.56187	1.07175	2.06448	0.68569	0.35664
0.45000	0.08823	0.20312	0.44711	0.90951	1.86072	0.68111	0.35599
0.50000	0.04765	0.13762	0.35801	0.79902	1.73178	0.67908	0.35574
0.56234	0.00375	0.06277	0.25374	0.66678	1.57496	0.67619	0.35538
0.75000		0.00280	0.11430	0.44675	1.27398	0.66548	0.35393
1.00000			0.03648	0.27540	0.98782	0.64691	0.35141
1.33352			0.00291	0.14531	0.70822	0.61538	0.34697
1.77828				0.05968	0.45016	0.56353	0.33924
3.16228				0.00123	0.09673	0.36965	0.30346
5.62341					0.00375	0.10830	0.21382
10.00000						0.00390	0.07200
17.78279							0.00272

converged for each result. To validate this numerical approach, we compared the numerical evaluations with the asymptotic solutions given by equations (40) and (45) for the case of $c_a = 1.0$, $\varepsilon = 1$, $x_0 = 0.5$, $\tau_0 = 10$, and at the point $x = 0.1$. Early in time, at $\tau = 0.01$, the small τ approximations give $W_s = 0.00995$, and $V_s = 0.00005$, while our computed results are $W = 0.00994$ and $V = 0.00005$. They are in excellent agreement for this small τ. Even at a modest value of $\tau = 0.1$, equation (45) predicts $W_s = 0.095$ and $V_s = 0.005$ whereas the numerical results are $W = 0.09531$ and $V = 0.00468$. They are still in good agreement if the accuracy of the calculation (accurate up to the fourth digit after the decimal point) and the errors in the asymptotic solutions (in τ^3) are considered. For large time, at $\tau = 100$, the asymptotic expression gives $W_a = 0.35494$ which differs from the numerical result $W = 0.35714$ by 0.62%. The agreement between W_a and W becomes better and better as we increase the value of τ. For example, at $\tau = 316.23$, the difference between the two reduces to 0.16%. Clearly, the numerical results match the asymptotic solutions where they are appropriate and thus validate the asymptotic approximations and the numerical scheme for the double integrals at least to some extent.

Table 2. Material energy density, $V(x,\tau)$, for the case with $\varepsilon = 1$, $c_a = 1$, $\tau_0 = 10$, $x_0 = 0.5$. The upper section is diffusion solution and the lower section is transport solution

$x\backslash\tau$	0.10000	0.31623	1.00000	3.16228	10.0000	31.6228	100.000
0.01000	0.00466	0.03816	0.21859	0.75342	1.75359	0.67926	0.35554
0.10000	0.00464	0.03768	0.21565	0.74557	1.74218	0.67885	0.35548
0.17783	0.00458	0.03658	0.20913	0.72837	1.71726	0.67796	0.35536
0.31623	0.00424	0.03253	0.18765	0.67348	1.63837	0.67517	0.35497
0.45000	0.00315	0.02476	0.15298	0.58978	1.51991	0.67100	0.35438
0.50000	0.00234	0.02042	0.13590	0.55041	1.46494	0.66907	0.35411
0.56234	0.00137	0.01515	0.11468	0.50052	1.39405	0.66640	0.35374
0.75000	0.00023	0.00580	0.06746	0.37270	1.19584	0.65656	0.35235
1.00000		0.00139	0.03173	0.24661	0.96571	0.63947	0.34988
1.33352		0.00015	0.01063	0.13729	0.71412	0.61022	0.34555
1.77828			0.00210	0.05918	0.46369	0.56166	0.33797
3.16228				0.00281	0.09834	0.37513	0.30294
5.62341					0.00306	0.11060	0.21452
10.00000						0.00334	0.07269
17.78279							0.00258
0.01000	0.00468	0.04093	0.27126	0.94670	2.11186	0.70499	0.35914
0.10000	0.00468	0.04093	0.26839	0.93712	2.09585	0.70452	0.35908
0.17783	0.00468	0.04093	0.26261	0.91525	2.06052	0.70348	0.35895
0.31623	0.00468	0.04032	0.23978	0.84082	1.94365	0.70020	0.35854
0.45000	0.00455	0.03314	0.18826	0.70286	1.74291	0.69532	0.35793
0.50000	0.00234	0.02046	0.14187	0.60492	1.61536	0.69308	0.35766
0.56234	0.00005	0.00635	0.08838	0.48843	1.46027	0.68994	0.35728
0.75000		0.00005	0.03014	0.30656	1.16591	0.67850	0.35581
1.00000			0.00625	0.17519	0.88992	0.65868	0.35326
1.33352			0.00017	0.08352	0.62521	0.62507	0.34875
1.77828				0.02935	0.38688	0.57003	0.34086
3.16228				0.00025	0.07642	0.36727	0.30517
5.62341					0.00253	0.10312	0.21377
10.00000						0.00342	0.07122
17.78279							0.00261

Two cases were chosen to be calculated: a purely absorbing medium ($c_a = 1.0$) and one where half the opacity is from scattering ($c_a = 0.5$). Other parameters, specifying the media and the sources for the two cases, are $\varepsilon = 1$, $x_0 = 0.5$, and $\tau_0 = 10$. For each case, W and V were computed at different (x, τ) points and the results are tabulated in Tables 1–4, respectively. Most of the tabulated points are equally spaced logarithmically in time and space. A few space points are added to resolve the spatial structure of the radiation source. For all the numbers in the tables, there are at least four digits of accuracy. Most tabulated points required only a few minutes of computation time. However, some points, especially those near the front of the wave propagation, had bad sign cancellation and required a large number integrand evaluations and equivalently a much longer computation time to converge. All the 216 transport solutions in the tables were calculated on a low-end desk-top workstation (Macintosh 7100) and took roughly 100 hours of computing.

In addition to the transport benchmark results, we also list in Tables 1–4 the benchmark results of the classic diffusion approximation to the same problem under consideration. The diffusion benchmark was generated exactly following the procedure

Table 3. Radiation energy density, $W(x,\tau)$, for the case with $\varepsilon = 1$, $c_a = 0.5$, $\tau_0 = 10$, $x_0 = 0.5$. The upper section is diffusion solution and the lower section is transport solution

$x\backslash\tau$	0.10000	0.31623	1.00000	3.16228	10.0000	31.6228	100.000
0.01000	0.09624	0.25861	0.55843	1.02657	1.89725	0.66231	0.35317
0.10000	0.09544	0.25480	0.55147	1.01724	1.88569	0.66192	0.35311
0.17783	0.09339	0.24629	0.53618	0.99683	1.86044	0.66107	0.35299
0.31623	0.08415	0.21763	0.48708	0.93197	1.78051	0.65840	0.35261
0.45000	0.06222	0.16989	0.41139	0.83380	1.66052	0.65441	0.35203
0.50000	0.04879	0.14590	0.37546	0.78793	1.60483	0.65257	0.35176
0.56234	0.03256	0.11638	0.33032	0.72942	1.53294	0.65002	0.35139
0.75000	0.00781	0.05532	0.22027	0.57428	1.33105	0.64063	0.35002
1.00000	0.00066	0.01749	0.12237	0.41099	1.09447	0.62432	0.34758
1.33352		0.00274	0.05100	0.25563	0.83191	0.59646	0.34330
1.77828			0.01332	0.12888	0.56382	0.55030	0.33582
3.16228			0.00005	0.01031	0.14284	0.37344	0.30122
5.62341				0.00002	0.00703	0.11874	0.21397
10.00000						0.00490	0.07380
17.78279							0.00293
0.01000	0.09757	0.29363	0.72799	1.28138	2.26474	0.68703	0.35675
0.10000	0.09757	0.29365	0.71888	1.26929	2.24858	0.68656	0.35668
0.17783	0.09758	0.29364	0.69974	1.24193	2.21291	0.68556	0.35654
0.31623	0.09756	0.28024	0.63203	1.15018	2.09496	0.68235	0.35618
0.45000	0.09033	0.21573	0.50315	0.98599	1.89259	0.67761	0.35552
0.50000	0.04878	0.14681	0.40796	0.87477	1.76426	0.67550	0.35527
0.56234	0.00383	0.06783	0.29612	0.74142	1.60822	0.67252	0.35491
0.75000		0.00292	0.13756	0.51563	1.30947	0.66146	0.35346
1.00000			0.04396	0.33319	1.02559	0.64239	0.35092
1.33352			0.00324	0.18673	0.74721	0.61024	0.34646
1.77828				0.08229	0.48739	0.55789	0.33868
3.16228				0.00160	0.11641	0.36631	0.30281
5.62341					0.00554	0.11177	0.21323
10.00000						0.00491	0.07236
17.78279							0.00296

described in a previous work (Su and Olson, 1996), with the Marshak boundary condition replaced with a reflective boundary condition. Omitting the details, we simply give the diffusion solutions for the radiation and material energy densities for this problem to be

$$W_{\mathrm{d}}(x,\tau) = \frac{1}{\pi x_0}\int_0^1 \mathrm{d}\eta \sin(\beta x_0)\cos(\beta x)\left\{\frac{3}{\beta^2\eta}(\mathrm{e}^{-c_{\mathrm{a}}\eta^2\tau^*} - \mathrm{e}^{-c_{\mathrm{a}}\eta^2\tau}) + \frac{1}{c_{\mathrm{a}}\eta[1+\varepsilon(1-\eta^2)]^2}(\mathrm{e}^{-\gamma\tau^*} - \mathrm{e}^{-\gamma\tau})\right\}, \tag{46}$$

$$V_{\mathrm{d}}(x,\tau) = W_{\mathrm{d}}(x,\tau) - \frac{1}{\pi x_0}\int_0^1 \mathrm{d}\eta \sin(\beta x_0)\cos(\beta x)\left\{\frac{\mathrm{e}^{-\gamma\tau^*} - \mathrm{e}^{-\gamma\tau} - \mathrm{e}^{-c_{\mathrm{a}}\eta^2\tau^*} + \mathrm{e}^{-c_{\mathrm{a}}\eta^2\tau}}{c_{\mathrm{a}}\eta[1+\varepsilon(1-\eta^2)]}\right\}, \tag{47}$$

Table 4. Material energy density, $V(x,\tau)$, for the case with $\varepsilon = 1$, $c_{\mathrm{a}} = 0.5$, $\tau_0 = 10$, $x_0 = 0.5$. The upper section is diffusion solution and the lower section is transport solution

$x \setminus \tau$	0.10000	0.31623	1.00000	3.16228	10.0000	31.6228	100.000
0.01000	0.00241	0.02100	0.14040	0.61433	1.66211	0.69022	0.35698
0.10000	0.00240	0.02074	0.13852	0.60802	1.65110	0.68977	0.35692
0.17783	0.00236	0.02013	0.13435	0.59419	1.62705	0.68879	0.35680
0.31623	0.00219	0.01789	0.12066	0.54998	1.55086	0.68571	0.35640
0.45000	0.00163	0.01362	0.09865	0.48236	1.43632	0.68113	0.35581
0.50000	0.00121	0.01126	0.08783	0.45047	1.38311	0.67901	0.35553
0.56234	0.00071	0.00837	0.07438	0.41007	1.31458	0.67608	0.35515
0.75000	0.00012	0.00323	0.04425	0.30691	1.12417	0.66530	0.35373
1.00000		0.00078	0.02114	0.20529	0.90356	0.64666	0.35121
1.33352			0.00723	0.11666	0.66890	0.61500	0.34679
1.77828			0.00147	0.05214	0.43608	0.56305	0.33906
3.16228				0.00287	0.09748	0.36959	0.30339
5.62341					0.00381	0.10867	0.21390
10.00000						0.00385	0.07215
17.78279							0.00270
0.01000	0.00242	0.02255	0.17609	0.77654	2.00183	0.71860	0.36067
0.10000	0.00242	0.02253	0.17420	0.76878	1.98657	0.71805	0.36065
0.17783	0.00242	0.02256	0.17035	0.75108	1.95286	0.71687	0.36047
0.31623	0.00242	0.02223	0.15520	0.69082	1.84104	0.71312	0.36005
0.45000	0.00235	0.01826	0.12164	0.57895	1.64778	0.70755	0.35945
0.50000	0.00121	0.01128	0.09194	0.49902	1.52383	0.70499	0.35917
0.56234	0.00003	0.00350	0.05765	0.40399	1.37351	0.70144	0.35876
0.75000		0.00003	0.01954	0.25610	1.09216	0.68851	0.35727
1.00000			0.00390	0.14829	0.83248	0.66637	0.35465
1.33352			0.00009	0.07161	0.58640	0.62937	0.35004
1.77828				0.02519	0.36629	0.57001	0.34200
3.16228				0.00018	0.07658	0.36066	0.30553
5.62341					0.00290	0.10181	0.21308
10.00000						0.00385	0.07077
17.78279							0.00273

where

$$\beta = \eta\sqrt{3c_a\left[\varepsilon + \frac{1}{(1-\eta^2)}\right]}, \qquad \gamma = c_a\left[1 + \frac{1}{\varepsilon(1-\eta^2)}\right], \qquad \tau^* = \max\left[0, (\tau - \tau_0)\right].$$

These diffusion solutions are much easier to be evaluated numerically than the transport solutions. The reason for giving the diffusion results is to show the difference between the transport solution and the diffusion solution, which is the lowest order approximation to the transport solution. Any reasonable code (either S_n or P_n) should predict results between the two solutions.

In order to visualize the numerical results and the difference between the transport solution and the diffusion one, Figs 1 and 2 show the evolution of the radiation and material energy densities, respectively, for the purely absorbing case. The radiation energy density is shown as a linear plot in order to emphasize the behavior near the symmetry plane. Clearly the difference between transport and diffusion theories is significant when the source is on. Especially near $\tau = 10$ and $x = 0$, diffusion theory predicts results about 20% lower than the correct ones, that of transport theory. At large times, with no internal driving source, the radiation field relaxes to the equilibrium diffusion solution. Figure 2 shows the material energy density on a logarithmic scale so that one can see the advancement of the wave front. As one would expect, the diffusion solution allows radiation to propagate too quickly. Energy gets out ahead of the distance allowed by light travel time considerations. Late in time, the two solutions converge.

CONCLUSION

In this paper we considered the non-equilibrium radiative transfer in an infinite, homogeneous, and isotropically scattering medium, with an internal radiation source. The analytical solution to this problem was constructed by using the Laplace transform with respect to the temporal variable and the Fourier transform with respect to the spatial variable. This approach is able to treat the integration over angular variable exactly. The source considered here is isotropic and uniformly distributed in a finite space during a finite period of time, but the method also applies to other types of sources and even to anisotropically scattering cases. For the radiation and material energy contents, very simple expressions, in elementary functions, were obtained. It is found that these energy contents are independent of the angular and spatial distribution of the source. For the radiation and material energy fields in the medium, which are essential to validate numerical solution algorithms used in codes, the transport solutions, as functions of space and time, were given in the form of double integrals. These solutions were evaluated numerically and compared with the diffusion benchmark results.

It should be emphasized that the purpose of this work is to provide a complete transport benchmark for non-equilibrium radiative transfer. The problem we considered is mathematically simpler than that considered by Ganapol and Pomraning (1983). However, the two problems have the same usefulness and serve the same practical purpose, i.e. to confirm quantitatively the numerical schemes employed in codes. The essential difference between the two problems, when used to validate codes, is only the type of boundary condition.

The Marshak wave problem considered by Ganapol and Pomraning (1983) has a isotropic flux-type boundary condition whereas our problem is equivalent to a half-space one with a reflective boundary condition. We hope the data given here will be useful in code development for time-dependent radiation transport. We finally comment that the interior solution of the half-space Marshak wave problem could be obtained in a similar way by

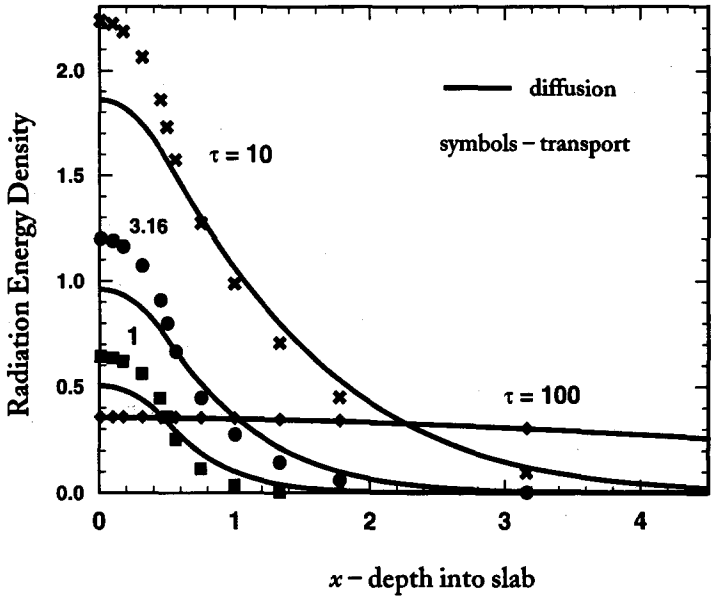

Fig. 1. The diffusion and transport solutions for the radiation energy density are shown as functions of position at different times, as labeled.

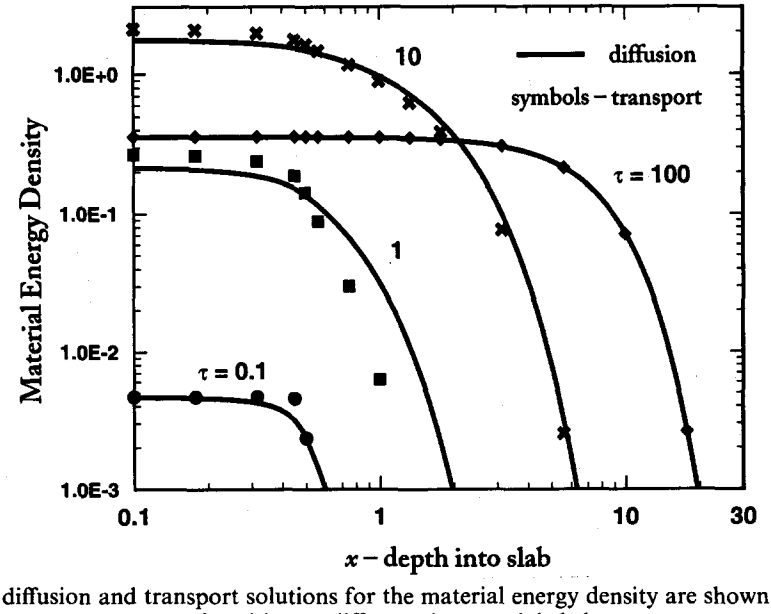

Fig. 2. The diffusion and transport solutions for the material energy density are shown as functions of position at different times, as labeled.

applying the transform method described in this work, since the exiting solution to the problem is known (Ganapol and Pomraning, 1983). This represents possible work for the future.

Acknowledgements—This work was performed under the auspices of the U.S. Department of Energy by Los Alamos National Laboratory. The authors are indebted to Professor B. D. Ganapol for valuable comments and suggestions leading to an improved presentation of this work.

REFERENCES

Case, K. M. (1960) *Annals of Physics*, **9**, 1.

Case, K. M., Hoffmann, F. and Placzek, G. (1953) *Introduction to the Theory of Neutron Diffusion*, Vol. 1. Los Alamos National Laboratory, Los Alamos, New Mexico.

Case, K. M. and Zweifel, P. F. (1967) *Linear Transport Theory*. Addison-Wesley, Reading, MA.

Ganapol, B. D. (1979) *Journal of Quantitative Spectroscopy and Radiative Transfer* **22**, 135.

Ganapol, B. D. and Pomraning, G. C. (1983) *Journal of Quantitative Spectroscopy and Radiative Transfer* **29**, 311.

Kuščer, I. and Zweifel, P. F. (1965) *Journal of Mathematical Physics*, **6**, 1125.

Marshak, R. E. (1958) *The Physics of Fluids* **1**, 24.

Papmehl, N. (1966) *Nucl. Sci. Engng* **24**, 307.

Pomraning, G. C. (1979) *Journal of Quantitative Spectroscopy and Radiative Transfer* **21**, 249.

Pomraning, G. C. and Shokair, I. R. (1981) *Journal of Quantitative Spectroscopy and Radiative Transfer* **25**, 325.

Press, W. H., Teukolsky, S. A., Vetterling, W. T. and Flannery, B. P. (1992) *Numerical Recipes in Fortran*, 2nd ed. Cambridge University Press, New York.

Su, B. and Olson, G. L. (1996) *Journal of Quantitative Spectroscopy and Radiative Transfer* **56**, 337.